TISSUE ENGINEERING: Part A
Volume 19, Numbers 3 and 4, 2013

DOI: 10.1089/ten.tea.2012.0257

Recombinant Fibronectin Matrix Mimetics Specify Integrin Adhesion and Extracellular Matrix Assembly

Daniel C. Roy, MS,[1] and Denise C. Hocking, PhD[1,2]

Tissue engineering seeks to create functional tissues and organs by integrating natural or synthetic scaffolds with bioactive factors and cells. Creating biologically active scaffolds that support key aspects of tissue regeneration, including the re-establishment of a functional extracellular matrix (ECM), is a challenge currently facing this field. During tissue repair, fibronectin is converted from an inactive soluble form into biologically active ECM fibrils through a cell-dependent process. ECM fibronectin promotes cell processes critical to tissue regeneration and regulates the deposition and organization of other ECM proteins. We previously developed biomimetics of ECM fibronectin by directly coupling the heparin-binding fragment of the first type III repeat of fibronectin (FNIII1H) to the integrin-binding repeats (FNIII8–10). As adhesive substrates, fibronectin matrix mimetics promote cell growth, migration, and contractility through a FNIII1H-dependent mechanism. Here, we analyzed fibronectin matrix mimetic variants designed to include all or part of the integrin-binding domain for their ability to support new ECM assembly. We found that specific modifications of the integrin-binding domain produced adhesive substrates that selectively engage different integrin receptors to, in turn, regulate the amount of fibronectin and collagen deposited into the ECM. The ability of fibronectin matrix mimetics to direct cell–substrate interactions and regulate ECM assembly makes them promising candidates for use as bioactive surfaces, where precise control over integrin-binding specificity and ECM deposition are required.

Introduction

Fibronectin is a principal component of interstitial matrices, where it contributes to both the structural integrity and biological function of tissues and organs.[1] Fibronectin is a dimeric glycoprotein, composed of two nearly identical polypeptides that are joined at their C-termini by disulfide bonds.[2] In turn, each fibronectin monomer is composed of homologous, individually folded modules, designated type I, II, or III, based on the folding pattern.[1] Fibronectin interacts with a variety of cell-surface receptors and extracellular matrix (ECM) proteins through specific binding domains, including the amino-terminal matrix assembly domain (FNI1–5), a central cell-binding domain (FNIII8–10), the collagen/gelatin-binding domain (FNI6-I9), and several heparin-binding domains.[3] The primary cell adhesive activity of fibronectin has been localized to the integrin-binding sequence, Arg-Gly-Asp (RGD), which is located in an exposed loop situated between 2 β strands of FNIII10.[4] The RGD sequence of fibronectin interacts with several different integrin receptors, including α5β1 and αvβ3 integrins.[3] Additional amino acid sequences in neighboring modules contribute to the affinity and specificity of integrin receptor binding.[3,5]

Fibronectin exists in a soluble form in the plasma and in an insoluble, fibrillar form in the ECM. The conversion of soluble fibronectin into ECM fibrils is an active, cell-dependent process.[6] Fibronectin matrix assembly is initiated by the binding of the amino-terminal matrix assembly domain of fibronectin to cell-surface receptors within focal contacts.[6,7] α5β1 integrins bound to fibronectin subsequently translocate away from focal contacts and into fibrillar adhesions by a tensin-dependent mechanism.[8] This translocation along the axis of the actin cytoskeleton exerts forces on bound fibronectin that extend the molecule to expose otherwise cryptic, self-association sites within the central type III modules.[8–10] Binding of soluble fibronectin to these newly exposed sites likely contributes to the lateral and longitudinal growth of fibronectin fibrils,[6,11] ultimately leading to the formation of a disulfide-stabilized fibronectin matrix.[12]

The assembly of a fibronectin matrix stimulates cell and tissue processes critical to tissue regeneration. In the body, fibronectin is rapidly upregulated in response to tissue injury, while decreased fibronectin levels have been associated with nonhealing wounds.[13,14] Conversely, aberrant fibronectin matrix deposition can lead to fibrotic diseases, resulting in impairment of organ function.[15] The ECM form of fibronectin specifically promotes cell spreading,[16] growth,[17]

Departments of [1]Biomedical Engineering and [2]Pharmacology and Physiology, University of Rochester School of Medicine and Dentistry, Rochester, New York.

migration,[18] and contractility.[19] Fibronectin matrices also serve as scaffolds for ECM proteins and growth factors.[20,21] Fibronectin matrix assembly promotes collagen matrix deposition,[22,23] organization,[19] and tensile strength,[24] and is also required for the deposition of fibrinogen,[25] fibrillin,[26] fibulin,[27] and tenascin C[28] into the ECM. In turn, fibronectin matrix assembly stimulates microtissue formation on native collagen gels,[29] supports assembly of endothelial neovessels,[30] and controls vascular tone in the skeletal muscle.[31] Together, these studies highlight the importance of fibronectin matrix assembly in establishing a functional ECM that can direct tissue repair and regeneration.

In earlier studies, we localized the bioactivity of ECM fibronectin to a matricryptic heparin-binding site in FNIII1.[16,18,31,32] Though buried in soluble fibronectin,[32–34] this matricryptic site becomes exposed during the matrix assembly process or as a result of tension exerted by cells on fibronectin fibrils.[10,31] We engineered fibronectin matrix mimetics that directly couple the open heparin-binding FNIII1 fragment (FNIII1H) to the integrin-binding domain (FNIII8–10) to provide cells with regulatory signals similar to those from ECM fibronectin.[32,35] We have shown that as adhesive substrates, the fibronectin matrix mimetics GST/III1H,8–10, GST/III1H,8,10, and GST/III1H,8^{RGD} support cell spreading, growth, migration, and contractility to a similar or greater extent than full-length fibronectin.[35]

Smart biomaterials are currently being engineered in an attempt to generate tissues and organs *in vitro*. Examples include the perfusion-decellularized whole organs to generate intact ECM scaffolds that anatomically mimic native tissue. Perfusion-decellularized scaffolds are then repopulated with cells to produce metabolically functional organs, including hearts, livers, and lungs.[36] At present, these cell-based engineered tissues show limited survival and function *in vivo*.[36] Tissue and organ survival may be enhanced through the use of novel adhesive coating materials that stimulate cells to produce a new, native ECM that in turn, is capable of promoting cell functions critical for tissue homeostasis. In the present study, we assessed the ability of several recombinant fibronectin matrix mimetics to support cell-dependent ECM deposition, and then determined the structural and proliferative capacity of the newly formed fibronectin matrices.

Materials and Methods

Recombinant proteins, reagents, and cells

A schematic of the recombinant fibronectin proteins is shown in Figure 1A. GST/III1H,8–10, GST/III1H,8,10, GST/III1H,8^{RGD}, GST/III1H, and FNIII11C were produced in *Escherichia coli* and purified as described.[32,35,37] The R1R2 peptide was produced by synthesis of an artificial gene (Integrated DNA Technologies) encoding amino acids Gly^{195}-Thr^{253} (bases 694–870) from the bacterial adhesin protein, SFS.[38] NcoI and PstI restriction sites were engineered on the 5′ and 3′ ends of the SFS sequence by addition of a 5′ Met and 3′ Ala-Gly, respectively. The protein sequence was cloned into the pEcoli-Cterm 6xHN plasmid (Clontech Laboratories), expressed in *E. coli* and purified over Ni-Sepharose. Human plasma fibronectin was isolated from Cohn's fraction I and II.[39] Alexa^{488}-labeled fibronectin was made by incubating plasma fibronectin with Alexa Fluor® 488 tetrafluorophenyl (TFP) ester (Life Technologies); unreacted dye was removed by size exclusion chromatography. Type I collagen was from BD Biosciences. Fluorescein isothiocyanate (FITC)-collagen I was from United States Biological. Fibronectin polyclonal, α-tubulin monoclonal (clone

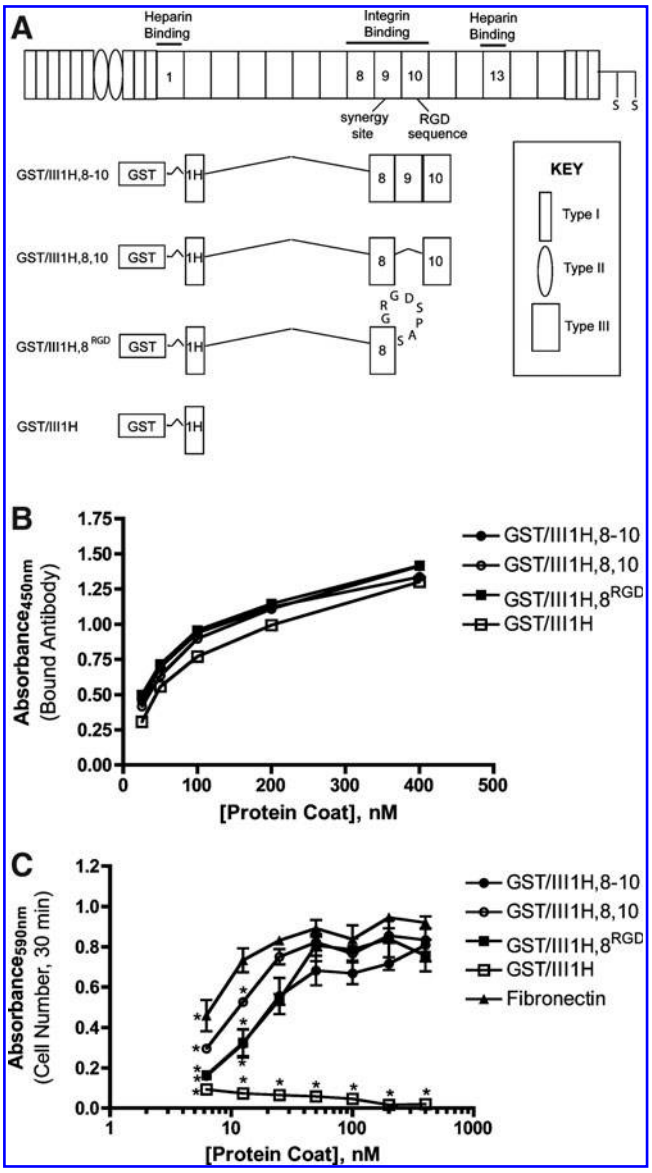

FIG. 1. Analysis of protein surface adsorption and cell adhesion. **(A)** Schematic representation of a fibronectin subunit and fibronectin matrix mimetics. **(B)** Tissue culture plates were coated with increasing concentrations of proteins. The relative amount of protein bound to wells was determined by enzyme-linked immunosorbent assay. **(C)** Tissue culture plates were precoated with fibronectin matrix mimetics or full-length fibronectin at concentrations ranging from 6.25 nM to 400 nM. The number of adherent cells was determined as described in Methods. Data are presented as mean absorbance of triplicate wells ± standard error of the mean (SEM) and represent one of three experiments. *Significantly different from 12.5 nM fibronectin, $p < 0.05$; GST/III1H,8–10, GST/III1H,8,10, and GST/III1H,8^{RGD} were not different at concentrations >50 nM (analysis of variance [ANOVA]).

DM1A), and vinculin monoclonal (clone VIN-11-5) antibodies were obtained from Sigma; horseradish peroxidase-conjugated (HRP) goat anti-mouse and goat anti-rabbit antibodies were from Bio-Rad (Hercules, CA); α5 (clone 5H10–27), αv (clone H9.2B8), β1 (clone Ha2/5), and β3 (clone 2C9.G2) integrin function-blocking monoclonal antibodies and IgG and IgM controls were from BD Biosciences; The β5 integrin function-blocking monoclonal antibody (clone KN52) was from eBioscience; the glutathione S-transferase (GST) monoclonal antibody (clone DG122-2A7), the fibronectin monoclonal antibody (clone CCBD), and α5 integrin polyclonal antibodies (AB1921 and AB1928) were from Millipore; Alexa-labeled secondary antibodies and Alexa Fluor 488 phalloidin were from Life Technologies; Bis[sulfosuccinimidyl] suberate (BS^3) was from Thermo Fisher Scientific. Tissue culture supplies were from Corning/Costar. Chemical reagents were from J.T. Baker or Sigma.

Mouse embryonic fibronectin-null fibroblasts (FN-null MEFs; provided by Dr. Jane Sottile, University of Rochester, Rochester, NY) were cultured at 37°C with 8% CO_2 on collagen I-coated dishes under fibronectin- and serum-free conditions using a 1:1 mixture of Cellgro® (Mediatech) and Aim V (Life Sciences).[17] Human mesenchymal stem cells (MSCs) and the MSC Growth Medium were from Lonza. The MesenCult®-XF Serum-free Medium was from STEMCELL Technologies. MSCs were cultured at 37°C with 5% CO_2 using MSC Growth Media and were used between passage two and five. Tissue culture plates were coated with recombinant fibronectin proteins or full-length fibronectin diluted in phosphate-buffered saline (PBS) at the indicated concentrations for 90 min at 37°C. The unbound protein was removed and wells were washed with PBS before seeding cells.

Solid-phase enzyme-linked immunosorbent assay

Tissue culture plates (96-well) were incubated with fibronectin matrix mimetics at indicated concentrations, washed with PBS, and blocked with 1% bovine serum albumin in Tris-buffered saline (TBS). Bound proteins were detected using an anti-GST monoclonal antibody followed by HRP-conjugated goat anti-mouse secondary antibodies. Wells were washed with TBS and the assay was developed using o-phenylenediamine dihydrochloride. The absorbance at 450 nm was measured with a microplate spectrophotometer (Bio-Rad).

Cell adhesion assays

FN-null MEFs (1.5×10^5 cells/mL) were seeded on tissue culture plates (96-well) precoated with fibronectin matrix mimetics or full-length fibronectin at indicated concentrations. Cells were allowed to adhere for 30 min at 37°C, washed with PBS, and then fixed with 1% paraformaldehyde. Cells were stained with 0.5% crystal violet, solubilized in 1% sodium dodecyl sulfate (SDS), and the absorbance at 590 nm was measured.[40]

For integrin-blocking adhesion assays, FN-null MEFs (3×10^5 cells/mL) were preincubated in suspension with integrin function-blocking antibodies (25 μg/mL) for 45 min. Cells were seeded onto 96-well tissue culture plates (9.5×10^4 cells/cm^2) precoated with fibronectin matrix mimetics or fibronectin. For plates coated with GST/III1H,8–10, GST/III1H,8,10, and fibronectin, cells were centrifuged into contact with the adhesive substrate for 4 min at 700 rpm (70 × g force) at 4°C.[41] Wells were washed with PBS and adherent cells were fixed with 1% paraformaldehyde. Cells were stained with 0.5% crystal violet, solubilized in 1% SDS, and the absorbance at 590 nm was measured. For plates coated with GST/III1H,8^{RGD}, cells were allowed to adhere for 30 min at 4°C. Plates were washed with PBS and adherent cells were counted manually.

Immunofluorescence microscopy

FN-null MEFs were seeded onto tissue culture plates (35 mm) precoated with recombinant fibronectin proteins or fibronectin, and incubated for 4 h at 37°C to allow for cell adhesion and spreading. Cells were either fixed with 2% paraformaldehyde and processed for immunofluorescence microscopy,[32] or treated with full-length fibronectin (10 μg/mL) and cultured for an additional 20 h before fixation. Plates were incubated with the fibronectin polyclonal antibody, the α5 integrin monoclonal antibody (5H10–27), or the vinculin monoclonal antibody (VIN-11-5). MSCs were passaged with trypsin and resuspended in the MesenCult-XF Serum-free Medium. Cells were seeded onto 35-mm plates precoated with fibronectin proteins, cultured for 20 h, and then fixed with a 1:1 mixture of acetone and methanol. Fibronectin fibrils were visualized using anti-fibronectin monoclonal antibodies (clone CCBD) and costained with α5 integrin polyclonal antibodies (AB1928). The bound antibody was detected with either the goat anti-rabbit, goat anti-rat, or goat-anti mouse Alexa-labeled secondary antibody. Alexa Fluor 488 phalloidin was used to visualize actin. Cells were visualized with an Olympus BX60 microscope and images were obtained using a Spot digital camera (Diagnostic Instruments) or a EXi Blue Fluorescence Microscopy Camera (QImaging).

Fibronectin and collagen assays

FN-null MEFs were seeded at 3.0×10^4 cells/cm^2 onto tissue culture plates (48-well) precoated with recombinant fibronectin proteins (400 nM) and allowed to spread for 4 h. Cells were then treated with fibronectin (10 μg/mL) and incubated an additional 20 h at 37°C, 8% CO_2. Wells were washed with PBS to remove unbound fibronectin. Cells and matrix were extracted with reducing the SDS sample buffer[42] and lysates were analyzed by SDS-polyacrylamide gel electrophoresis (PAGE) and immunoblotting using enhanced chemiluminescence (Thermo Fisher Scientific).[19]

To quantify fibronectin deposition using fluorimetry, FN-null MEFs were seeded (3.0×10^4 cells/cm^2) on black-walled 96-well tissue culture plates precoated with recombinant fibronectin proteins or collagen I at indicated concentrations. Cells were allowed to spread for 4 h at 37°C, and then treated with $Alexa^{488}$-labeled fibronectin (FN^{488}, 10 μg/mL). To quantify collagen I deposition, adherent cells were treated with FITC-labeled collagen I (10 μg/mL) in either the absence or presence of fibronectin (10 μg/mL). In some studies, fibronectin (10 μg/mL) and FITC-labeled collagen (10 μg/mL) were incubated in the presence of either R1R2 (250 nM) or FNIII11C (250 nM) for 1 h before being added to cells. FN-null MEFs were incubated for 20 h at 37°C, 8% CO_2, and then washed with PBS. Methanol was added to wells and fluorescence intensity was quantified by exciting wells at 485 nm

and detecting sample emission at 528 nm using a Synergy H4 Multi-Mode Microplate Reader (BioTek).

Integrin crosslinking assays

FN-null MEFs (3.0×10^4 cells/cm^2) were seeded onto tissue culture plates (12-well) precoated with recombinant fibronectin proteins or fibronectin. Cells were incubated for 4 h at 37°C to allow for adhesion and spreading. Cell-surface proteins were crosslinked to the underlying substrate with 2.5 mM BS^3 (Thermo Fisher Scientific) in PBS for 30 min at 4°C before quenching the unreacted crosslinker with 50 mM Tris. Cells were extracted for 5 min on ice with 0.1% SDS, 2 mM PMSF, and 0.8 mg/mL Complete™ Protease Inhibitor Cocktail, ethylenediaminetetraacetic acid (EDTA)-free (Roche Diagnostics). Plates were washed with cold PBS and crosslinked proteins were solubilized in reducing SDS sample buffer. Samples were analyzed by SDS-PAGE and immunoblotting as described.[19]

Cell proliferation assays

Cell proliferation assays were performed as described previously.[17,35] Tissue culture plates (48-well) were precoated with recombinant fibronectin proteins or collagen I at the indicated concentrations. FN-null MEFs were seeded at 2.5×10^3 cells/cm^2 and incubated for 4 h at 37°C to allow for adhesion and spreading. Cells were then treated with either fibronectin (10 μg/mL) or an equal volume of PBS, incubated for 4 days at 37°C, 8% CO_2, then washed with PBS, and fixed with 1% paraformaldehyde. Cells were stained with 0.5% crystal violet, solubilized in 1% SDS, and the absorbance at 590 nm was measured.

Statistical analysis

Data are presented as mean ± standard error of the mean and are either compiled from three experiments or represent one of at least three experiments, each performed in either triplicate or quadruplicate. Statistical comparisons were performed using one-way analysis of variance followed by the Bonferroni post-test, with GraphPad Prism Version 4 software. Differences were considered significant for p-values less than 0.05.

Results

Fibronectin matrix mimetics as integrin-specific adhesive substrates

Enzyme-linked immunosorbent assays (ELISAs) were performed on tissue culture plates coated with increasing concentrations of the fibronectin matrix mimetics to compare coating densities among substrates. As shown in Figure 1B, coating density profiles were nearly identical for all of the fibronectin mimetics tested. Cell adhesion assays were performed to examine the ability of cells to adhere to the various substrates. FN-null MEFs, which do not produce endogenous fibronectin and are cultured under serum-free conditions, were utilized in these and subsequent studies to directly compare cellular responses to the fibronectin matrix mimetics versus full-length fibronectin. Cell adhesion to plates coated with GST/III1H,8–10, GST/III1H,8,10, or GST/III1H,8^{RGD} was similar at coating concentrations equal to or greater than 50 nM, and not significantly different from that observed on plates coated with 12.5 nM fibronectin (Fig. 1C). As expected, cells did not adhere to wells coated with GST/III1H, which does not contain a known integrin-binding sequence[35] (Fig. 1C).

Various function-blocking anti-integrin antibodies were then tested for their ability to block FN-null MEF attachment to tissue culture wells coated with the various fibronectin matrix mimetics. Blocking antibodies directed against α5, αv, β1, and β3 integrins were examined, as these integrin subunits are expressed by FN-null MEFs[17] and bind to full-length fibronectin at sites within the FNIII8–10 domain.[3] EDTA was used as a positive control to inhibit all integrin-mediated adhesion to the substrate. In the presence of either α5 or β1 integrin-blocking antibodies, cell adhesion to GST/III1H,8–10-coated plates was reduced by 51.0% ± 9.5% and 86.5% ± 3.2%, respectively, compared to control wells (Fig. 2A). In contrast, anti-αv, -β3, or -β5 integrin antibodies had no effect on cell adhesion to GST/III1H,8–10 (Fig. 2A), indicating that α5β1 integrins mediate adhesion to this substrate. Cell adhesion to GST/III1H,8,10, which lacks FNIII9 and the α5β1 integrin-binding synergy site,[5] was reduced with antibodies directed against integrin subunits α5 (by 28.8% ± 10.9%), αv (by 49.8% ± 7.8%), β1 (by 71.0% ± 6.3%), and β3 (by 30.5% ± 10.7%) (Fig. 2B), indicating that cell adhesion to GST/III1H,8,10 is mediated through a combination of α5β1, αvβ3, and potentially αvβ1 integrins. Cell adhesion to GST/III1H,8^{RGD} was inhibited with either αv or β3 integrin-blocking antibodies, by 82.7% ± 7.1% and 85.2% ± 6.1%, respectively (Fig. 2C). In contrast, anti-α5 or anti-β1 integrin antibodies had no effect on cell adhesion to GST/III1H,8^{RGD}, indicating that αvβ3 integrins alone mediate adhesion to GST/III1H,8^{RGD} (Fig. 2C). In comparison, cell adhesion to fibronectin was reduced only with α5 (by 53.0% ± 11.5%) and β1 (by 71.3% ± 4.0%) integrin-blocking antibodies, indicating that α5β1 integrins mediate adhesion to the fibronectin substrate (Fig. 2D). Thus, cell adhesion to both full-length fibronectin and the fibronectin matrix mimetic containing the complete cell-binding domain (GST/III1H,8–10) is mediated by α5β1 integrins. Removal of FNIII9 (GST/III1H,8,10) results in cell adhesion via a combination of α5β1 and αvβ3 integrins. Further reducing the cell-binding domain by removing FNIII10 and inserting the GRGDSP loop into FNIII8 (GST/III1H,8^{RGD}) results in cell adhesion that is mediated by αvβ3 integrins exclusively.

Fibronectin matrix assembly by cells adherent to synthetic matrix mimetics

Previous studies have shown that various adhesive substrates, including cell-binding fibronectin fragments, can either support or inhibit the cell-dependent assembly of a fibronectin matrix.[43–45] To assess the effects of fibronectin matrix mimetic substrates on the ability of cells to subsequently assemble a fibronectin matrix, fibronectin fibril formation by FN-null MEFs was visualized using immunofluorescence microscopy. FN-null MEFs assemble exogenously added, soluble fibronectin into ECM fibrils by mechanisms similar to those of fibronectin-expressing cells.[17] α5β1 integrin-specific substrates (GST/III1H,8–10 and fibronectin) did not support the assembly of a fibrillar fibronectin matrix (Fig. 3b, h). In contrast, fibronectin matrix mimetic

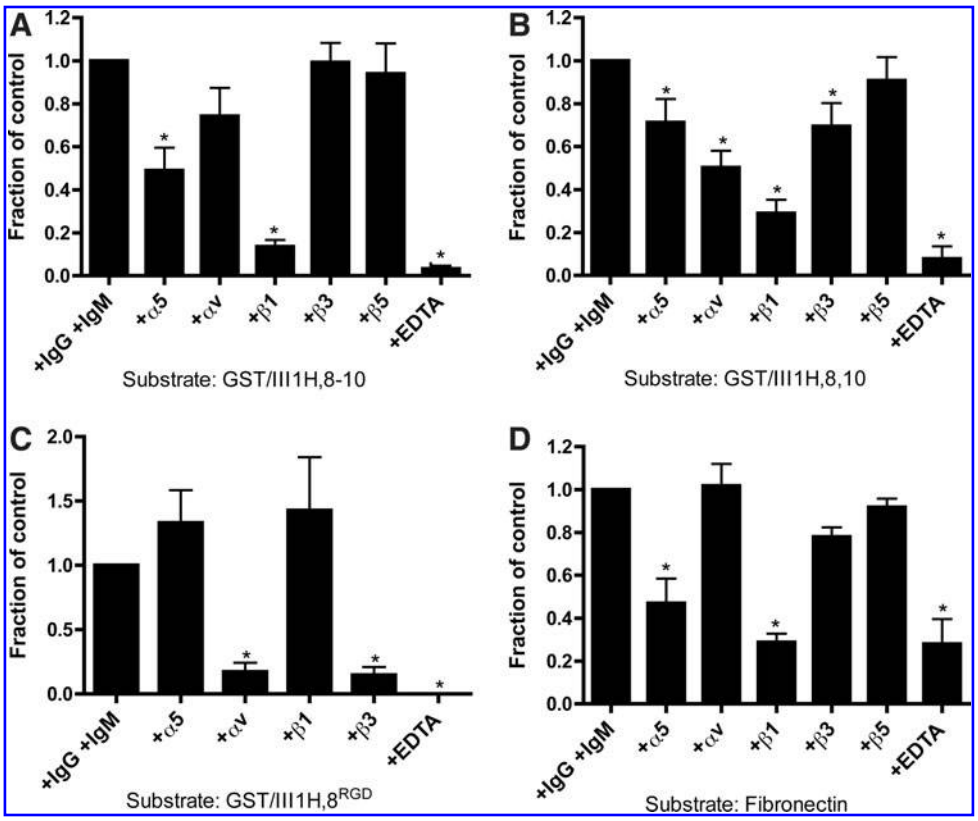

FIG. 2. Selective integrin-mediated adhesion to fibronectin matrix mimetics. Fibronectin-null mouse embryonic fibroblasts (FN-null MEFs) were seeded onto tissue culture plates precoated with 400 nM GST/III1H,8–10 **(A)**, GST/III1H,8,10 **(B)**, GST/III1H,8^{RGD} **(C)**, or 10 nM full-length fibronectin **(D)**, in the presence of integrin function-blocking antibodies, isotype-matched control antibodies (+IgG +IgM), or EDTA. Cell adhesion was determined as described in Methods. Data are compiled from three separate experiments each performed in triplicate. Values are represented as mean fold difference from +IgG +IgM control ± SEM. *Significantly different from +IgG +IgM, $p < 0.05$ (ANOVA). ETDA, ethylenediaminetetraacetic acid.

substrates that bind to cells via αvβ3 integrins (GST/III1H,8,10 and GST/III1H,8^{RGD}) supported fibronectin fibril formation (Fig. 3d, f).

Fibronectin binding and deposition by FN-null MEFs adherent to fibronectin matrix mimetic substrates was quantified by immunoblot analysis of cell/matrix lysates. Consistent with the immunofluorescence images shown in Figure 3, fibronectin was absent from lysates of cells adherent to the α5β1 integrin-binding substrate, GST/III1H,8–10, but present in lysates from cells adherent to αvβ3-binding substrates (Fig. 4A). Interestingly, fibronectin deposition by cells adherent to the fibronectin matrix mimetic substrate that binds solely via αvβ3 integrins (GST/III1H,8^{RGD}) was approximately two-fold greater compared with cells adherent to GST/III1H,8,10 (Fig. 4B), which binds to cells through both αvβ3 and α5β1 integrins. The amount of α-tubulin present in the lysates was similar in all groups (Fig. 4A), indicating that differences in fibronectin accumulation were not due to differences in cell number.

Exogenous fibronectin deposition was also assessed by quantifying the accumulation of Alexa^{488}-labeled fibronectin by cells adherent to the various matrix mimetics. Similar to results shown in Figure 4B, fibronectin accumulation by cells adherent to the αvβ3-binding substrates, GST/III-1H,8,10 and GST/III1H,8^{RGD}, was significantly greater compared with cells adherent to GST/III1H,8–10 (Fig. 4C). In addition, the amount of fibronectin deposited by cells adherent to GST/III1H,8^{RGD} was approximately twice that of cells adherent to GST/III1H,8,10 (Fig. 4C). Fluorescence intensity of cell-free, FN^{488}-treated wells was negligible for all substrates (Fig. 4C), indicating that FN^{488} does not bind directly to the protein substrates. Taken together, these data indicate that (i) cells adherent to GST/III1H,8–10 do not assemble a fibronectin matrix, and (ii) cells adherent to the αvβ3 integrin-specific substrate, GST/III1H,8^{RGD}, incorporate significantly more fibronectin into a fibrillar matrix than cells adherent to GST/III1H,8,10, the α5β1 and αvβ3 integrin-binding substrate.

ECM collagen I deposition by cells adherent to fibronectin matrix mimetics

The deposition of collagen I into the ECM is dependent on the coassembly of a fibronectin matrix.[22] To determine if fibronectin matrix mimetics that promote fibronectin matrix assembly also support collagen I deposition, FN-null MEFs adherent to saturating densities of fibronectin matrix mimetics were incubated with FITC-labeled collagen I for 20 h, in the absence or presence of soluble fibronectin. In the absence of fibronectin, FN-null MEFs adherent to the various matrix mimetics did not bind FITC-collagen I (Fig. 5A; "+cells, −FN"). Similarly, FITC-collagen I did not bind to the matrix mimetic substrates in the absence of cells (Fig. 5A; "−cells, −FN"), indicating that FITC-collagen does not bind directly to the protein-coated plates. In the presence of soluble fibronectin, cells adherent to GST/III1H,8–10 showed limited collagen I deposition 20 h after treatment (Fig. 5A; "+cells, +FN"). In contrast, GST/III1H,8,10- and GST/III1H,8^{RGD}-coated substrates supported collagen I deposition by cells in the presence of fibronectin (Fig. 5A). Moreover, GST/III1H,8^{RGD}-adherent cells showed a nearly two-fold increase in fibronectin-mediated collagen I deposition compared to cells adherent to GST/III1H,8,10 (Fig. 5A), which correlates well with the two-fold difference in fibronectin deposition observed with these two substrates (Fig. 4).

FN-null MEFs adherent to GST/III1H,8,10 or GST/III1H,8^{RGD} displayed collagen fibrils that colocalized

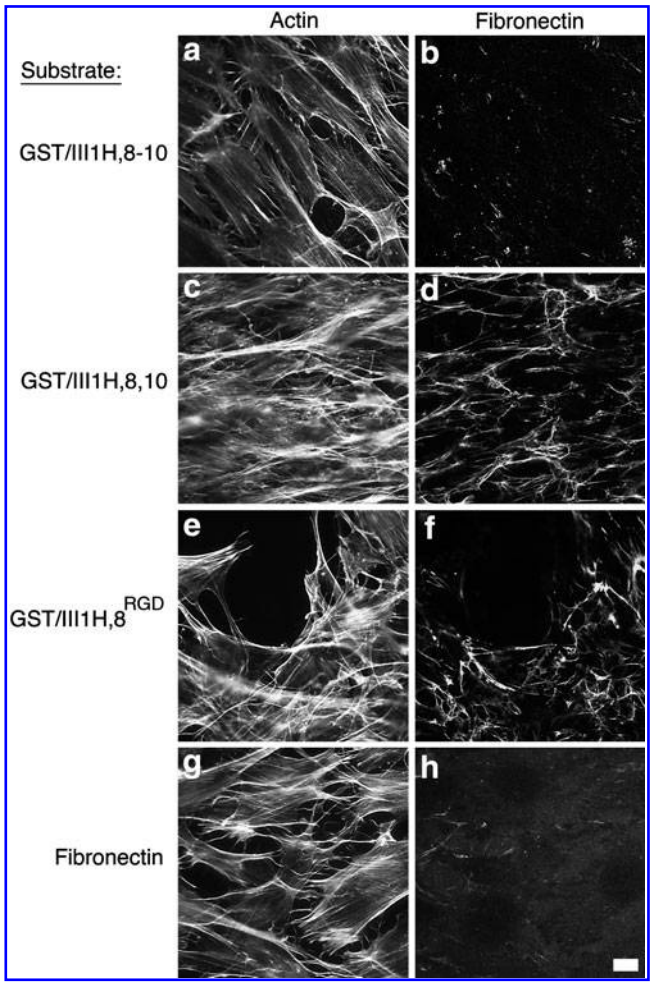

FIG. 3. αvβ3-binding substrates support fibronectin matrix assembly**.** FN-null MEFs were seeded (3.0×10^4 cells/cm^2) onto tissue culture plates precoated with fibronectin matrix mimetics [(**a–f**); 400 nM] or plasma fibronectin [(**g, h**); 10 nM]. Four hours after seeding, fibronectin (10 μg/mL) was added to each well and cells were incubated for an additional 20 h. Cells were processed for immunofluorescence microscopy as described in Methods. Fibronectin fibrils were visualized using polyclonal anti-fibronectin antibodies. Actin was visualized using Alexa^{488}-labeled phalloidin. Images represent one of three experiments. Bar = 10 μm.

extensively with fibronectin fibrils (Fig. 5B). To determine whether the interaction of collagen with fibronectin was required for collagen deposition, FITC-collagen I and fibronectin were coincubated in the presence of the R1R2 peptide, a protein fragment that inhibits fibronectin–collagen interactions without affecting fibronectin matrix assembly.[46] Addition of R1R2 blocked FITC-collagen I deposition by cells adherent to either GST/III1H,8,10 or GST/III1H,8^{RGD} substrates (Fig. 5C). Coincubation of fibronectin and FITC-collagen I with the control fragment, FNIII11C,[46] had no effect on FITC-collagen I incorporation (Fig. 5C). These data indicate that fibronectin is required for collagen I deposition by cells adherent to fibronectin matrix mimetic substrates. Further, the αvβ3 integrin-binding substrate, GST/III1H,8^{RGD}, supports increased fibronectin and collagen I deposition into the ECM compared to substrates that have an α5β1 integrin-binding component (GST/III1H,8–10 and GST/III1H,8,10).

α5β1 integrin ligation and translocation by cells adherent to matrix mimetic substrates

Upon binding of soluble fibronectin to the cell surface, α5β1 integrins translocate centripetally from focal adhesions into mature matrix adhesions.[8] Our data indicate that GST/III1H,8–10 mediates cell adhesion through α5β1 integrins, but does not support fibronectin matrix assembly. Thus, we reasoned that αvβ3 integrin-binding substrates (GST/III1H,8,10 and GST/III1H,8^{RGD}) may allow for α5β1 integrin translocation into matrix adhesions during the matrix assembly process, whereas on the GST/III1H,8–10 substrate, α5β1 integrins remain in focal adhesions. To test this possibility, immunofluorescence microscopy was used to localize α5β1 integrins on cell surfaces following fibronectin fibril formation. α5β1 integrin-specific substrates, GST/III1H,8–10 (Fig. 6a, b) and fibronectin (Fig. 6g, h) did not support fibronectin fibril formation and showed punctate α5β1 integrins that appeared to localize to central and peripheral focal adhesions (Fig. 6; arrowheads). In contrast, α5β1 integrins colocalized with fibronectin fibrils in matrix adhesions (Fig. 6; arrows) of cells adherent to GST/III1H,8,10 (Fig. 6c, d) and GST/III1H,8^{RGD} (Fig. 6e, f). These data suggest that α5β1 integrin translocation into fibrillar adhesions takes place only on fibronectin matrix mimetic substrates that ligate cells, at least in part, via αvβ3 integrins.

Quantifying substrate-bound α5β1 integrins

Our studies, thus far, suggest that upon adhesion to GST/III1H,8–10, α5β1 integrins preferentially engage the adhesive substrate instead of soluble fibronectin, thus inhibiting the initiation of the matrix assembly process. To assess α5β1 integrin clustering solely in response to substrate adhesion, FN-null MEFs were allowed to adhere and spread for 4 h on plates precoated with saturating densities of the various fibronectin matrix mimetics in the absence of soluble fibronectin. α5β1 integrins were visualized by immunofluorescence microscopy. α5β1 integrins colocalized with vinculin in central and peripheral focal adhesions of cells adherent to both GST/III1H,8–10 (Fig. 7Aa–c) and full-length fibronectin (Fig. 7Aj–l). Cells adherent to GST/III1H,8,10 showed reduced α5β1 integrin clustering compared to GST/III1H,8–10, and α5β1 integrin-containing focal adhesions were localized primarily to the cell edge (Fig. 7Ad–f). Clustered α5β1 integrins were completely absent from cells adherent to GST/III1H,8^{RGD}, despite strong vinculin staining of focal adhesions at the periphery of cells (Fig. 7Ag–i).

Substrate-bound α5β1 integrins were isolated and quantified by treating adherent FN-null MEFs, in the absence of fibronectin, with a membrane-impermeable chemical crosslinker 4 h after seeding. In agreement with the immunofluorescence images shown in Figure 7A, significantly more α5β1 integrins bound to the GST/III-1H,8–10 substrate versus GST/III1H,8,10 and GST/III1H,8^{RGD} substrates (Fig. 7B–C). Interestingly, fewer α5β1 integrins bound to full-length fibronectin compared to GST/III1H,8–10 (Fig. 7B–C). This may be due, in part, to the fact that there is a 20-fold difference in the molar coating concentration of full-length fibronectin compared to GST/III1H,8–10. Together, these data

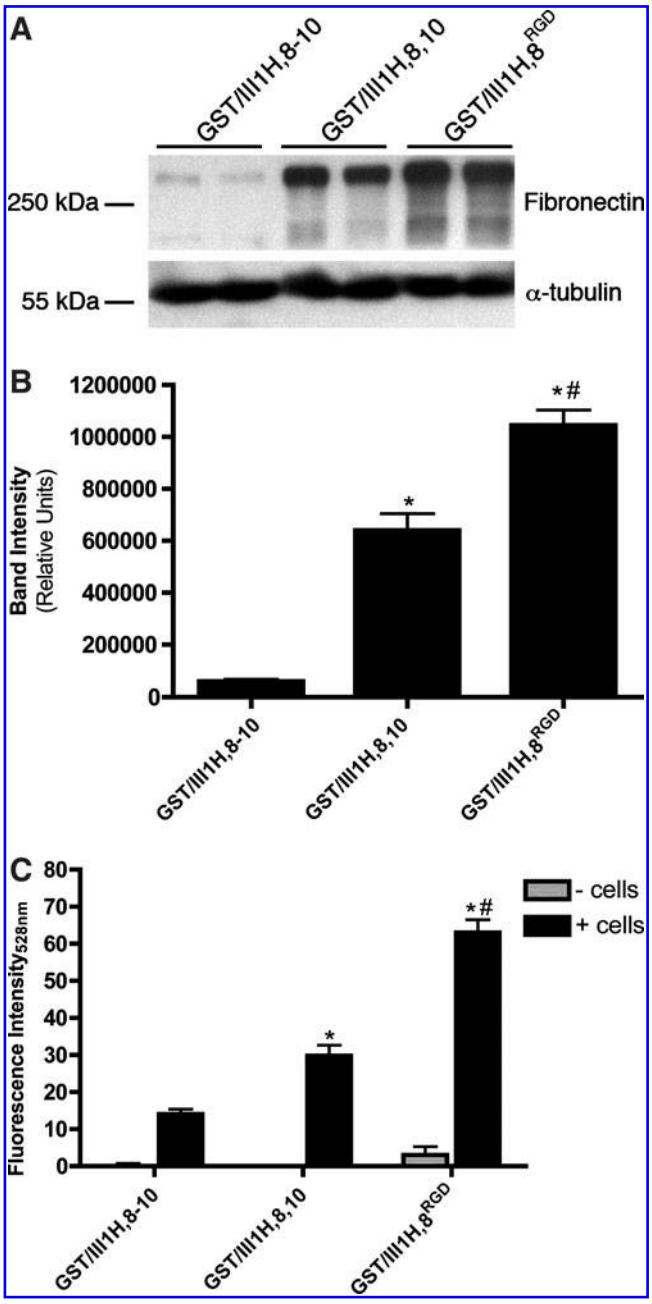

FIG. 4. Quantification of fibronectin matrix accumulation. FN-null MEFs were seeded (3.0×10^4 cells/cm^2) on tissue culture plates precoated with fibronectin matrix mimetics at 400 nM. Four hours after seeding, unlabeled **(A, B)** or Alexa^{488}-labeled **(C)** fibronectin (FN^{488}) was added at 10 μg/mL and cells were incubated for 20 h. **(A)** Immunoblot analysis of whole cell lysates using antibodies directed against fibronectin and α-tubulin. Immunoblot represents one of three experiments each performed in duplicate wells. **(B)** Fibronectin band intensities of immunoblots were quantified by densitometry. *Significantly different from GST/III1H,8–10, $p<0.05$. #Significantly greater than GST/III1H,8,10, $p<0.05$ (ANOVA). **(C)** FN^{488} accumulation was determined as described in Methods. Data are presented as mean fluorescence ± SEM and represent one of three experiments. *Significantly different from GST/III1H,8–10, $p<0.05$. #Significantly greater than GST/III1H,8,10, $p<0.05$ (ANOVA).

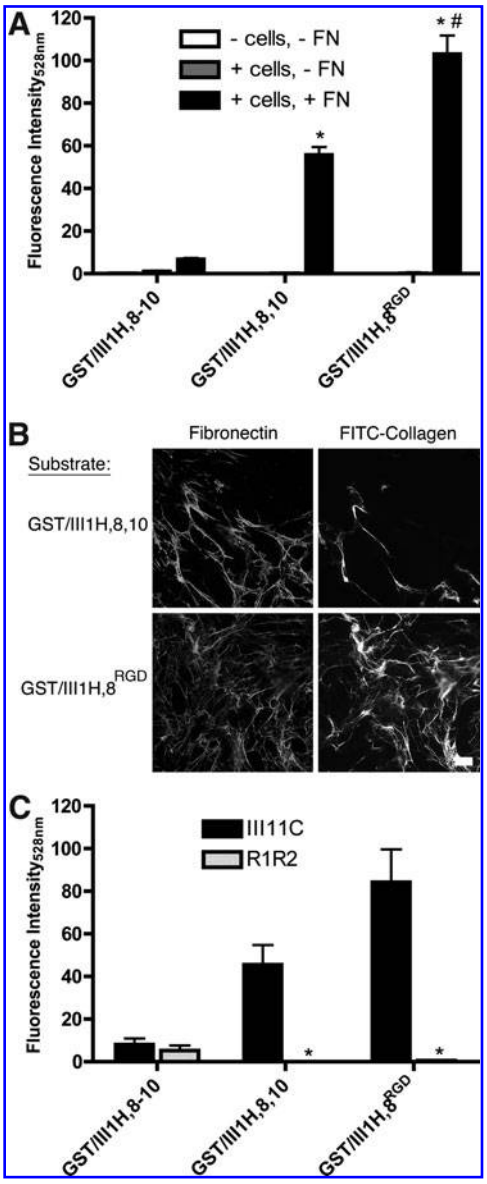

FIG. 5. Collagen I deposition by cells adherent to fibronectin matrix mimetics. FN-null MEFs were seeded (3.0×10^4 cells/cm^2) on tissue culture plates precoated with various matrix mimetics (400 nM). Four hours after seeding, cells were treated with fibronectin (10 μg/mL) and FITC-collagen I (10 μg/mL) for 20 h. In **(A)**, control wells received either fluorescein isothiocyanate (FITC)-collagen I only (+cell, −FN) or FITC-collagen I in the absence of both cells and fibronectin (-cells, –FN). FITC-collagen I binding was quantified as described in Methods. Data are presented as mean fluorescence intensity ± SEM and represent one of three experiments performed in quadruplicate. *Significantly different from GST/III1H,8–10, $p<0.05$. #Significantly greater than GST/III1H,8,10, $p<0.05$ (ANOVA). In **(B)**, cells were processed for immunofluorescence microscopy and stained using an antibody against fibronectin. Images represent one of three experiments. Bar = 10 μm. **(C)** Four hours after seeding, cells were treated with fibronectin (10 μg/mL) and FITC-collagen I (10 μg/mL) in the presence of either R1R2 (250 nM) or FNIII11C (250 nM). FITC-collagen I was quantified after 20 h. Data are presented as mean fluorescence +/- SEM and represent 1 of 3 experiments performed in quadruplicate. *Significantly different from FNIII11C treatment, $p<0.05$ (ANOVA).

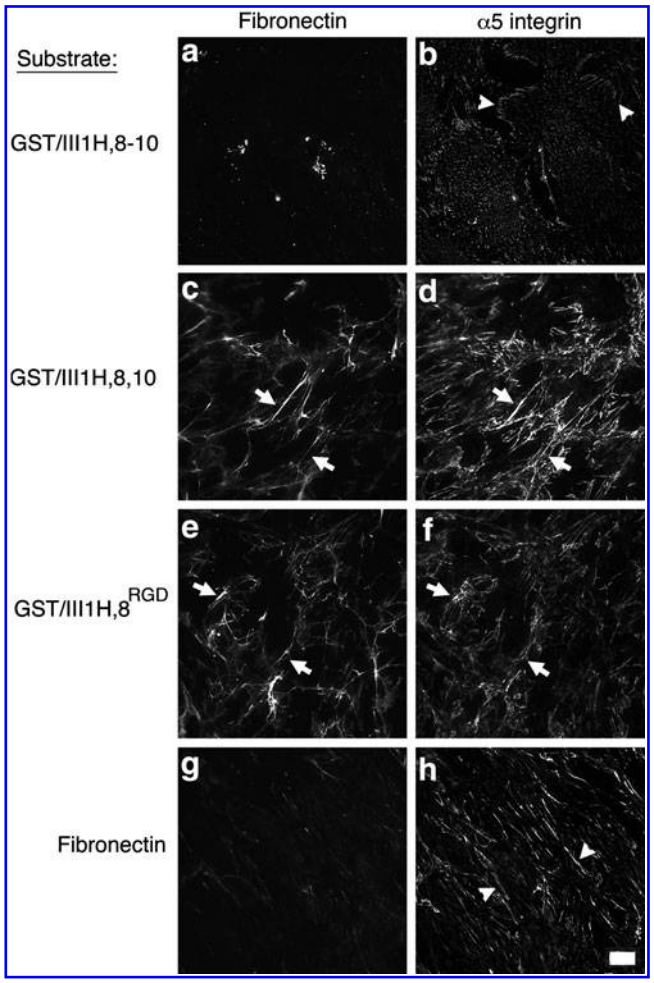

FIG. 6. α5β1 integrin translocation on αvβ3-binding substrates. FN-null MEFs were seeded (3.0×10^4 cells/cm^2) on tissue culture plates precoated with various fibronectin matrix mimetics [(**a**–**f**); 400 nM] or full-length fibronectin [(**g**, **h**); 10 nM]. Four hours after seeding, soluble fibronectin (10 μg/mL) was added to each well and cells were incubated for 20 h. Cells were processed for immunofluorescence microscopy and stained using antibodies directed against fibronectin and α5 integrin subunits. Arrows point to α5β1 integrins in matrix adhesions. Arrowheads point to α5β1 integrins in focal adhesions. Images represent one of three experiments. Bar = 10 μm.

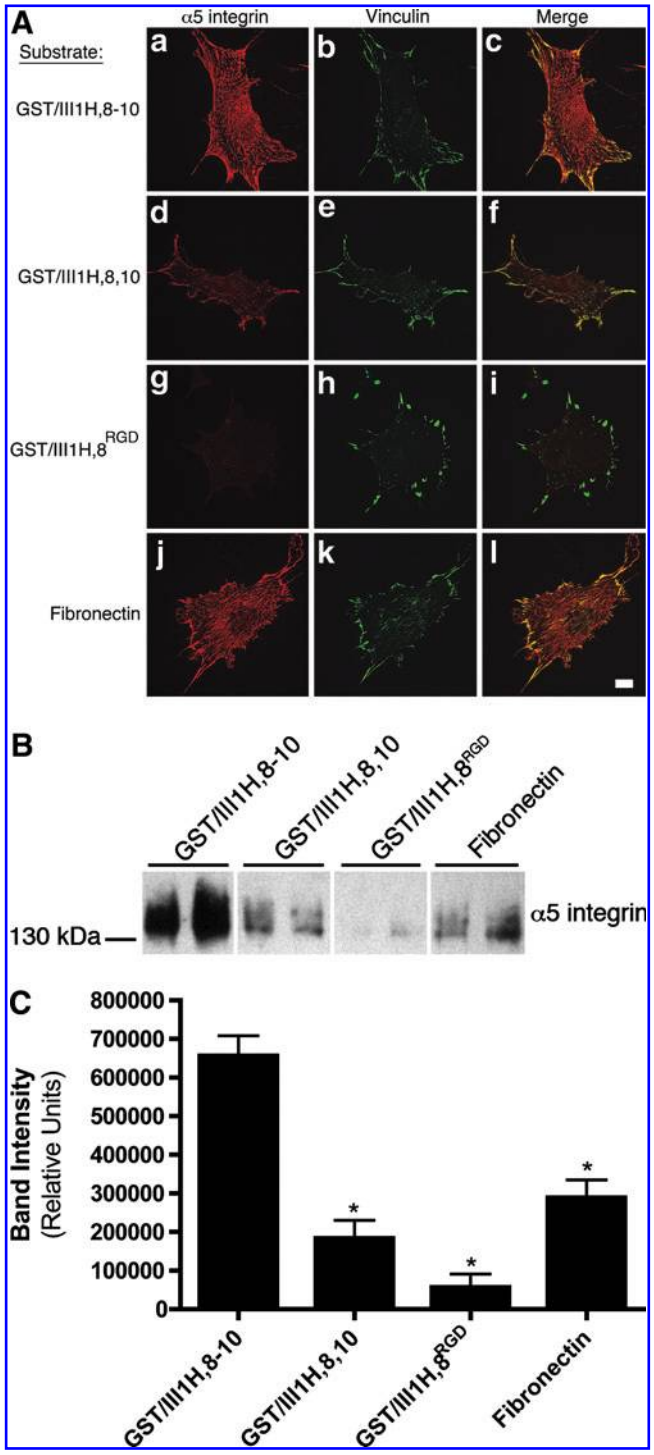

FIG. 7. Substrate-dependent ligation and clustering of α5β1 integrins. FN-null MEFs were seeded [**(A)** 2.5×10^3 cells/cm^2; **(B)** 3×10^4 cells/cm^2] onto tissue culture plates precoated with 400 nM of the various fibronectin matrix mimetics or 10 nM full-length fibronectin and allowed to adhere and spread for 4 h. **(A)** Cells adherent to matrix mimetics (**a-i**) or full-length fibronectin (**j-l**) were processed for immunofluorescence microscopy and stained using antibodies against α5 integrin and vinculin. Images represent one of three experiments. Bar = 10 μm. **(B)** Cell surface proteins bound to the adhesive substrates were crosslinked using BS^3. Unbound proteins were extracted and crosslinked α5β1 integrins were analyzed by immunoblotting. Immunoblot represents one of three experiments each performed in duplicate wells. **(C)** Band intensities of α5 integrin subunits were quantified and compiled from three separate experiments each performed in duplicate wells. *Significantly different from GST/III1H,8–10, $p<0.05$ (ANOVA).

indicate that removal of FNIII9 from GST/III1H,8–10 reduces the amount of substrate-bound α5β1 integrins.

To determine if the extent of α5β1 integrin ligation by the matrix mimetic substrate is a regulator of fibronectin matrix assembly, FN-null MEFs were seeded onto plates precoated with various concentrations of GST/III1H,8–10. Substrate-bound integrins were isolated 4 h after cell seeding and quantified. There were no observable differences in the ability of cells to adhere and spread at any of the coating concentrations used (data not shown). However, the amount

of substrate-bound α5β1 integrins was significantly reduced when plates were coated with lower concentrations of GST/III1H,8–10 (25 nM and 50 nM) compared to 400 nM GST/III1H,8–10 (Fig. 8A–B). To determine the relationship between the coating density of the α5β1 integrin-binding substrate and the ability of cells to assemble a fibronectin matrix, we asked whether decreasing the coating density of GST/III1H,8–10 and thus, reducing α5β1 integrin-substrate ligation, would allow for cell-dependent fibronectin matrix assembly. Indeed, cells adherent to 25 nM GST/III1H,8–10 assembled a fibronectin matrix with α5β1 integrins in fibrillar adhesions (Fig. 8Ca, b), whereas cells adherent to plates coated with 400 nM GST/III1H,8–10 did not assemble fibronectin fibrils and retained α5β1 integrins in focal adhesions (Fig. 8Cc, d). Taken together, these data provide evidence that modulating the number of binding sites for α5β1 integrins in the adhesive substrate directly affects α5β1 integrin translocation and the assembly of a fibronectin matrix.

Fibronectin matrix assembly and cell proliferation

To determine whether the fibronectin matrix formed by cells adherent to the different fibronectin matrix mimetics enhances cell proliferation, FN-null MEFs adherent to the various fibronectin matrix mimetics were treated with soluble fibronectin and the cell number was determined after 4 d. A protein-coating concentration of 50 nM was used in these studies to permit fibronectin matrix assembly by cells adherent to GST/III-1H,8–10. At this coating concentration, no significant differences in the amount of fibronectin deposited by cells adherent to GST/III1H,8–10, GST/III1H,8,10, or GST/III1H,8^{RGD} were observed (Fig. 9A). Consistent with previous results using collagen as the adhesive substrate,[17] collagen-adherent FN-null MEFs displayed a 2.06 ± 0.13-fold increase in the cell number on Day 4 in response to fibronectin compared to cells treated with the vehicle control, PBS (Fig. 9B). Cells adherent to the α5β1 integrin-binding substrate, GST/III1H,8–10, showed a 1.54 ± 0.10-fold increase in the cell number with fibronectin treatment over PBS-treated controls (Fig. 9B). Similarly, GST/III1H,8,10, the α5β1 and αvβ3 integrin-binding substrate, supported a 1.53 ± 0.12-fold increase in the cell number. Adhesion to the αvβ3 integrin-binding substrate, GST/III1H,8^{RGD}, resulted in a 2.90 ± 0.51-fold increase in the cell number in response to fibronectin over the vehicle control (Fig. 9B).

Fibronectin matrix assembly by MSCs

We next asked whether adhesion to the various fibronectin matrix mimetics influences fibronectin matrix assembly by fibronectin-expressing, human MSCs. MSCs are often incorporated into tissue-engineered scaffolds due to their ability to differentiate into bone, cartilage, and soft tissue.[47] MSCs were seeded onto plates precoated with fibronectin matrix mimetics and cultured for 20 h in serum-free growth media. Immunofluorescence microscopy was used to visualize fibronectin fibrils and α5β1 integrins. As observed with FN-null MEFs, MSCs adherent to the α5β1 integrin-binding substrate, GST/III1H,8–10, did not assemble a fibronectin matrix and α5β1 integrins remained clustered in focal contacts (Fig. 10a–c). In contrast, MSCs adherent to either GST/III1H,8,10 or GST/III1H,8^{RGD}, assembled endogenous fibronectin into fibrils that colocalized with α5β1 integrins (Fig. 10d–i). MSCs adherent to full-length fibronectin produced only a few fibronectin fibrils that localized to the

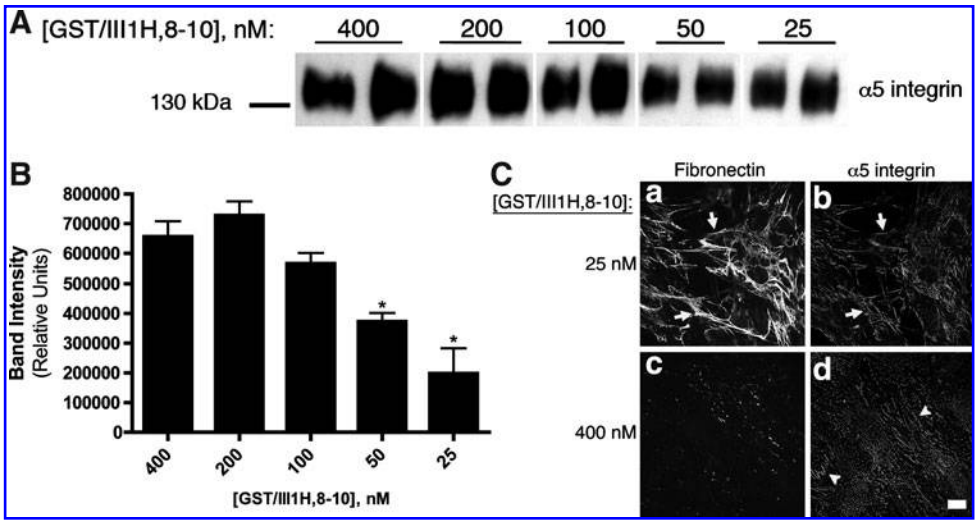

FIG. 8. Coating density of GST/III1H,8–10 controls fibronectin matrix assembly. FN-null MEFs were seeded (3.0×10^4 cells/cm^2) onto tissue culture plates precoated with GST/III1H,8–10 at indicated concentrations. **(A)** Four hours after seeding, cell surface proteins bound to the adhesive substrate were crosslinked using BS^3. Cells were extracted and bound proteins were analyzed by immunoblotting with an anti-α5 integrin antibody. Immunoblot represents one of three experiments each performed in duplicate wells. **(B)** α5 integrin band intensities were quantified and compiled from three separate experiments each performed in duplicate wells. *Significantly different from 400 nM GST/III1H,8–10, $p < 0.05$ (ANOVA). **(C)** Four hours after seeding, cells adherent to either 25 nM (**a,b**) or 400 nM (**c,d**) GST/III1H,8–10 were treated with fibronectin (10 μg/mL) and incubated an additional 20 h. Cells were processed for immunofluorescence microscopy and stained using antibodies against fibronectin and α5 integrins. Arrows point to α5β1 integrins in matrix adhesions. Arrowheads point to α5β1 integrins in focal adhesions. Images represent one of three experiments. Bar = 10 μm.

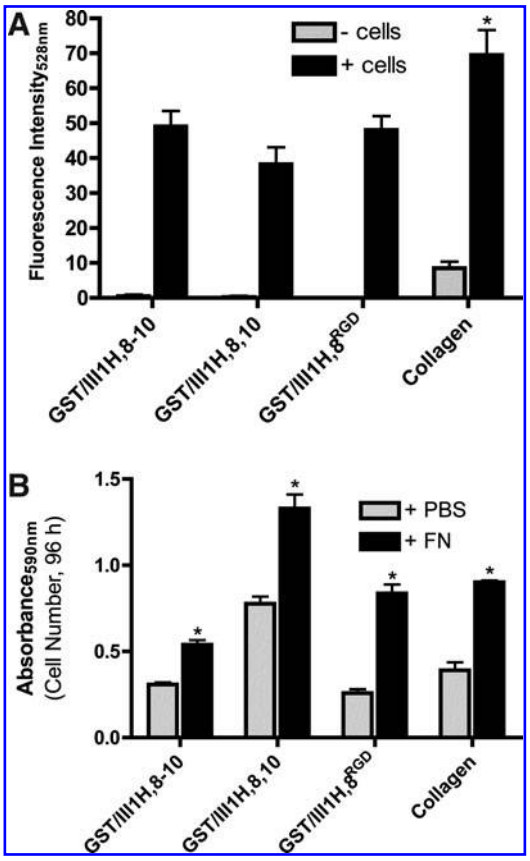

FIG. 9. Fibronectin-stimulated cell proliferation on matrix-supporting substrates. FN-null MEFs were seeded [**(A)** 3.0×10^4 cells/cm^2; **(B)** 2.5×10^3 cells/cm^2] on tissue culture plates precoated with matrix mimetics (50 nM) or collagen I (50 μg/mL). **(A)** Four hours after seeding, FN^{488} (10 μg/mL) was added and cells were incubated an additional 20 h. FN^{488} accumulation was quantified as described in Methods. Some wells received FN^{488} in the absence of cells (- cells) to assess fibronectin-substrate binding. Data are presented as mean fluorescence of quadruplicate wells ± SEM and represent one of three experiments. *Significantly greater than all other substrates, $p<0.05$ (ANOVA). **(B)** Four hours after seeding, fibronectin (10 μg/mL) or an equal volume of phosphate-buffered saline (PBS) was added and cells were incubated for 4 days. Cell number was determined as described in Methods. Data are expressed as mean absorbance of triplicate wells ± SEM and represent one of three experiments. *Significantly different from + PBS treatment, $p<0.05$ (ANOVA).

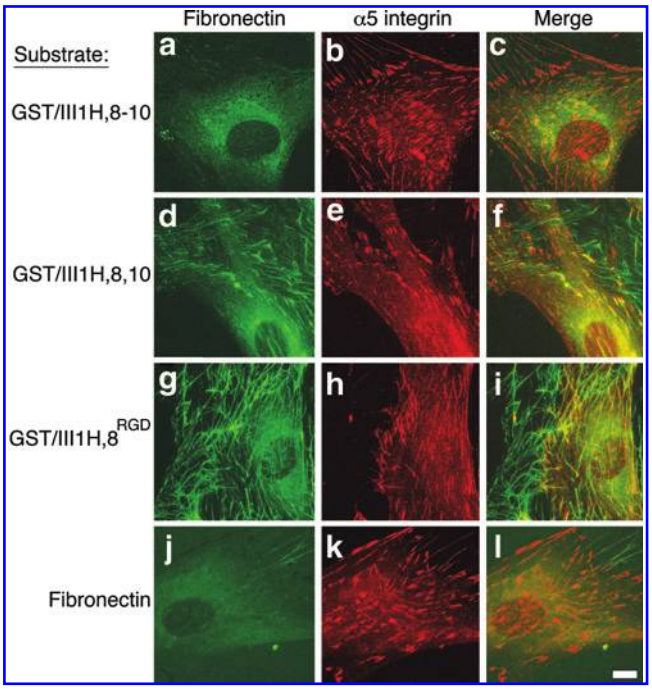

FIG. 10. Fibronectin matrix assembly by mesenchymal stem cells. Mesenchymal stem cells (MSCs) were seeded (2.5×10^3 cells/cm^2) on tissue culture plates precoated with various fibronectin matrix mimetics [(**a-i**); 400 nM] or full-length fibronectin [(**j-l**); 10 nM] and cultured for 20 h. Cells were processed for immunofluorescence microscopy and stained using antibodies directed against fibronectin and α5 integrin subunits. Images represent one of three experiments. Bar = 10 μm.

periphery of the cell (Fig. 10, panel j); α5β1 integrins were clustered in central and peripheral focal contacts throughout the cell (Fig. 10, panel k). These studies demonstrate that fibronectin matrix mimetic substrates are capable of directing fibronectin matrix assembly by MSCs.

Discussion

We have developed a series of fibronectin matrix mimetics by directly coupling the open, growth-promoting fragment of FNIII1 (FNIII1H) to various fragments spanning the integrin-binding domain (FNIII8–10). When used as adhesive substrates, fibronectin matrix mimetics promote cell spreading, proliferation, migration, and contractility.[35] Here, we report that modifications in the integrin-binding domain of the fibronectin matrix mimetics can be used to direct cell adhesion through either α5β1 or αvβ3 integrins and regulate fibronectin matrix deposition. Saturating densities of GST/III1H,8–10, the α5β1 integrin-binding substrate, retained α5β1 integrins in focal contacts and did not support the cell-mediated assembly of a fibronectin and collagen matrix. These results are consistent with previous reports that FNIII7–10 binds exclusively to α5β1 integrins[48] and does not support fibronectin matrix assembly.[43] In contrast, GST/III1H,8,10 bound cells through both α5β1 and αvβ3 integrins and supported fibronectin matrix assembly and collagen deposition. Inserting the RGD sequence from FNIII10 into the analogous region of FNIII8 (GST/III1H,8^{RGD}) produced a substrate that ligates αvβ3 integrins and supports elevated levels of fibronectin and collagen matrix deposition compared to the other matrix mimetics. Reducing the amount of substrate-bound α5β1 integrins by decreasing the coating density of GST/III1H,8–10 allowed for matrix assembly, providing evidence that the extent of α5β1 integrin ligation by the underlying adhesive substrate is a dominant regulator of ECM deposition.

In the present study, cell adhesion to full-length plasma fibronectin did not support fibronectin matrix assembly by either FN-null MEFs or MSCs (Figs. 3 and 10). Others have shown that substrates coated with plasma fibronectin at lower coating concentrations can support fibronectin matrix assembly.[43,44] However, at the higher fibronectin coating concentration used in the present study, α5β1 integrins

remained confined to focal contacts (Figs. 6 and 10). A direct relationship between fibronectin coating density and α5β1 integrin-mediated adhesive strength has been reported.[49] Thus, increased coating densities of plasma fibronectin may act as a dominant inhibitor of fibronectin matrix assembly. The conformation and mobility of the fibronectin substrate also impacts adhesion and fibrillogenesis. Fibronectin adsorbed onto tissue culture plastic, as in the current study, is in a conformation that exposes FNIII9–10 to in turn, increase α5β1 integrin-binding.[50] Others have shown that immobilizing fibronectin covalently to the underlying substrate confines α5β1 integrins within focal adhesions and reduces fibrillogenesis.[51] Thus, increasing α5β1 integrin–substrate interactions through a variety of mechanisms may reduce the pool of available integrins that can bind to soluble fibronectin and participate in ECM assembly.

The construct GST/III1H,8–10 contains an intact cell-binding domain and, similar to full-length fibronectin, bound cells via α5β1 integrins. Removal of FNIII9 from GST/III1H,8–10 to form GST/III1H,8,10 and GST/III1H,8^{RGD} resulted in either partial loss of α5β1 binding (GST/III1H,8,10; Fig. 2B) or total loss of α5β1 integrin binding (GST/III1H,8^{RGD}; Fig. 2C). This is likely due to loss of the Pro-His-Ser-Arg-Asn (PHSRN) sequence in FNIII9, which acts synergistically with the RGD sequence to bind α5β1 integrins.[5] Although mutating the PHSRN sequence in recombinant FNIII9–10 reduces α5β1 integrin-binding compared to intact FNIII9–10,[52] addition of FNIII8 to the mutated construct rescued the loss in α5β1 integrin binding, suggesting that FNIII8 can function much like FNIII9 to stabilize the interaction between FNIII10 and α5β1 integrins.[52] These data are consistent with the results of our integrin-blocking studies with GST/III1H,8,10, where the presence of both FNIII8 and FNIII10 supported α5β1 integrin adhesion independent of the PHSRN site in FNIII9. In our previous work,[35] GST/III1H,8–10 and GST/III1H,8,10, but not GST/III1H,8^{RGD}, supported high levels of cell migration. Taken together, these data suggest that highly migratory substrates should contain an α5β1 integrin-binding component.

Fibronectin matrix assembly by cells can increase the rate of cell proliferation.[17] Here, substrates that supported fibronectin ECM assembly also supported increased cell proliferation in response to fibronectin. GST/III1H,8–10 and GST/III1H,8,10, which have α5β1 integrin-binding components, both supported a 1.5-fold increase in cell number in response to fibronectin. The αvβ3 integrin-binding substrate, GST/III1H,8^{RGD}, supported a nearly 3-fold increase in cell number in response to fibronectin over PBS controls. Fibronectin matrix assembly by fibroblasts is mediated primarily by α5β1 integrins[6,8,11] and in our study, α5β1 integrins were found in fibrillar adhesions on all matrix-supporting constructs. Thus, the increased proliferative response to fibronectin by cells adherent to GST/III1H,8^{RGD} may be due to crosstalk between substrate-bound αvβ3 integrins and α5β1 integrins in fibrillar adhesions.[53] Dual-ligation of α5β1 and αvβ3 integrins may also account for the increase in cell growth in the absence of fibronectin on GST/III1H,8,10 compared to GST/III1H,8–10 (α5β1 integrin-mediated adhesion) and GST/III1H,8^{RGD} (αvβ3 integrin-mediated adhesion).

Small adhesion peptides, including those containing the RGD sequence, provide cells with a purified adhesive ligand, but typically fail to promote cell behaviors that are critical to tissue regeneration, including cell growth and differentiation.[48,54] Full-length ECM proteins provide a more natural adhesive substrate to cells, but do not provide integrin-specificity and moreover, do not reproduce the complex binding surfaces of native fibrillar ECMs.[55] Thus, novel adhesive substrates that both mimic native ECMs and provide for integrin specificity are currently being developed. To this end, fibronectin fragments, designed to promote α5β1 integrin ligation, enhance osteogenic differentiation of stromal cells and MSCs.[48,56] Similarly, myogenic differentiation can be induced on fibronectin-coated surfaces made to selectively ligate α5β1 integrins.[57] Materials with modified surface chemistries have also been used to trigger cell-free assembly of fibronectin matrices that in turn, drive myogenic differentiation.[58] Our approach has been to develop recombinant fibronectin matrix mimetics that combine the signaling capacity of ECM fibronectin with the production ease of small proteins. Fibronectin matrix mimetics containing the matricryptic site in FNIII1 promote cell behaviors critical to tissue repair, including growth, migration, and contractility. We now show that modifying the cell-binding domain of fibronectin matrix mimetics provides integrin-binding specificity and allows for control over ECM deposition. Thus, the use of fibronectin matrix mimetics as coating materials for scaffolds designed to generate tissue, whole organs, and stem cell niches is an exciting area of future research.

Acknowledgments

This work was supported by grant GM081513 from the National Institutes of Health. The authors thank Susan Wilke-Mounts and Sally Child for excellent technical assistance.

Disclosure Statement

No competing financial interests exist.

References

1. Hynes, R.O., and Yamada, K.M. Fibronectins: multifunctional modular glycoproteins. J Cell Biol **95,** 369, 1982.
2. Petersen, T.E., Thogersen, H.C., Skorstengaard, K., Vibe-Pedersen, K., Sahl, P., Sottrup-Jensen, L., *et al.* Partial primary structure of bovine plasma fibronectin: three types of internal homology. Proc Natl Acad Sci USA **80,** 137, 1983.
3. Pankov, R., and Yamada, K.M. Fibronectin at a glance. J Cell Sci **115,** 3861, 2002.
4. Potts, J.R., and Campbell, I.D. Fibronectin structure and assembly. Curr Opin Cell Biol **6,** 648, 1994.
5. Aota, S., Nomizu, M., and Yamada, K.M. The short amino acid sequence Pro-His-Ser-Arg-Asn in human fibronectin enhances cell-adhesive function. J Biol Chem **269,** 24756, 1994.
6. Magnusson, M.K., and Mosher, D.F. Fibronectin: structure, assembly, and cardiovascular implications. Arterioscler Thromb Vasc Biol **18,** 1363, 1998.
7. Dzamba, B.J., Bultmann, H., Akiyama, S.K., and Peters, D.M. Substrate-specific binding of the amino terminus of fibronectin to an integrin complex in focal adhesions. J Biol Chem **269,** 19646, 1994.
8. Pankov, R., Cukierman, E., Katz, B.Z., Matsumoto, K., Lin, D.C., Lin, S., *et al.* Integrin dynamics and matrix assembly: tensin-dependent translocation of alpha(5)beta(1) integrins

promotes early fibronectin fibrillogenesis. J Cell Biol **148,** 1075, 2000.
9. Baneyx, G., Baugh, L., and Vogel, V. Fibronectin extension and unfolding within cell matrix fibrils controlled by cytoskeletal tension. Proc Natl Acad Sci USA **99,** 5139, 2002.
10. Zhong, C., Chrzanowska-Wodnicka, M., Brown, J., Shaub, A., Belkin, A.M., and Burridge, K. Rho-mediated contractility exposes a cryptic site in fibronectin and induces fibronectin matrix assembly. J Cell Biol **141,** 539, 1998.
11. Mao, Y., and Schwarzbauer, J.E. Fibronectin fibrillogenesis, a cell-mediated matrix assembly process. Matrix Biol **24,** 389, 2005.
12. McKeown-Longo, P.J., and Mosher, D.F. Binding of plasma fibronectin to cell layers of human skin fibroblasts. J Cell Biol **97,** 466, 1983.
13. Herrick, S.E., Sloan, P., McGurk, M., Freak, L., McCollum, C.N., and Ferguson, M.W. Sequential changes in histologic pattern and extracellular matrix deposition during the healing of chronic venous ulcers. Am J Pathol **141,** 1085, 1992.
14. Hynes, R. Fibronectins. New York: Springer-Verlag; 1990.
15. To, W.S., and Midwood, K.S. Plasma and cellular fibronectin: distinct and independent functions during tissue repair. Fibrogenesis Tissue Repair **4,** 21, 2011.
16. Gui, L., Wojciechowski, K., Gildner, C.D., Nedelkovska, H., and Hocking, D.C. Identification of the heparin-binding determinants within fibronectin repeat III1: role in cell spreading and growth. J Biol Chem **281,** 34816, 2006.
17. Sottile, J., Hocking, D.C., and Swiatek, P.J. Fibronectin matrix assembly enhances adhesion-dependent cell growth. J Cell Sci **111,** 2933, 1998.
18. Hocking, D.C., and Chang, C.H. Fibronectin matrix polymerization regulates small airway epithelial cell migration. Am J Physiol Lung Cell Mol Physiol **285,** L169, 2003.
19. Hocking, D.C., Sottile, J., and Langenbach, K.J. Stimulation of integrin-mediated cell contractility by fibronectin polymerization. J Biol Chem **275,** 10673, 2000.
20. Sottile, J. Regulation of angiogenesis by extracellular matrix. Biochim Biophys Acta **1654,** 13, 2004.
21. Ruoslahti, E., Yamaguchi, Y., Hildebrand, A., and Border, W.A. Extracellular matrix/growth factor interactions. Cold Spring Harb Symp Quant Biol **57,** 309, 1992.
22. Sottile, J., and Hocking, D.C. Fibronectin polymerization regulates the composition and stability of extracellular matrix fibrils and cell-matrix adhesions. Mol Biol Cell **13,** 3546, 2002.
23. Velling, T., Risteli, J., Wennerberg, K., Mosher, D.F., and Johansson, S. Polymerization of type I and III collagens is dependent on fibronectin and enhanced by integrins alpha 11beta 1 and alpha 2beta 1. J Biol Chem **277,** 37377, 2002.
24. Gildner, C.D., Lerner, A.L., and Hocking, D.C. Fibronectin matrix polymerization increases tensile strength of model tissue. Am J Physiol Heart Circ Physiol **287,** H46, 2004.
25. Pereira, M., Rybarczyk, B.J., Odrljin, T.M., Hocking, D.C., Sottile, J., and Simpson-Haidaris, P.J. The incorporation of fibrinogen into extracellular matrix is dependent on active assembly of a fibronectin matrix. J Cell Sci **115,** 609, 2002.
26. Sabatier, L., Chen, D., Fagotto-Kaufmann, C., Hubmacher, D., McKee, M.D., Annis, D.S, *et al.* Fibrillin assembly requires fibronectin. Mol Biol Cell **20,** 846, 2009.
27. Twal, W.O., Czirok, A., Hegedus, B., Knaak, C., Chintalapudi, M.R., Okagawa, H., *et al.* Fibulin-1 suppression of fibronectin-regulated cell adhesion and motility. J Cell Sci **114,** 4587, 2001.
28. Chung, C.Y., Zardi, L., and Erickson, H.P. Binding of tenascin-C to soluble fibronectin and matrix fibrils. J Biol Chem **270,** 29012, 1995.
29. Sevilla, C.A., Dalecki, D., and Hocking, D.C. Extracellular matrix fibronectin stimulates the self-assembly of microtissues on native collagen gels. Tissue Eng Part A **16,** 3805, 2010.
30. Zhou, X., Rowe, R.G., Hiraoka, N., George, J.P., Wirtz, D., Mosher, D.F., *et al.* Fibronectin fibrillogenesis regulates three-dimensional neovessel formation. Genes Dev **22,** 1231, 2008.
31. Hocking, D.C., Titus, P.A., Sumagin, R., and Sarelius, I.H. Extracellular matrix fibronectin mechanically couples skeletal muscle contraction with local vasodilation. Circ Res **102,** 372, 2008.
32. Hocking, D.C., and Kowalski, K. A cryptic fragment from fibronectin's III1 module localizes to lipid rafts and stimulates cell growth and contractility. J Cell Biol **158,** 175, 2002.
33. Hocking, D.C., Sottile, J., and McKeown-Longo, P.J. Fibronectin's III-1 module contains a conformation-dependent binding site for the amino-terminal region of fibronectin. J Biol Chem **269,** 19183, 1994.
34. Briknarova, K., Akerman, M.E., Hoyt, D.W., Ruoslahti, E., and Ely, K.R. Anastellin, an FN3 fragment with fibronectin polymerization activity, resembles amyloid fibril precursors. J Mol Biol **332,** 205, 2003.
35. Roy, D.C., Wilke-Mounts, S.J., and Hocking, D.C. Chimeric fibronectin matrix mimetic as a functional growth- and migration-promoting adhesive substrate. Biomaterials **32,** 2077, 2011.
36. Song, J.J., and Ott, H.C. Organ engineering based on decellularized matrix scaffolds. Trends Mol Med **17,** 424, 2011.
37. Morla, A., Zhang, Z., and Ruoslahti, E. Superfibronectin is a functionally distinct form of fibronectin. Nature **367,** 193, 1994.
38. Lindmark, H., and Guss, B. SFS, a novel fibronectin-binding protein from Streptococcus equi, inhibits the binding between fibronectin and collagen. Infect Immun **67,** 2383, 1999.
39. Miekka, S.I., Ingham, K.C., and Menache, D. Rapid methods for isolation of human plasma fibronectin. Thromb Res **27,** 1, 1982.
40. Hocking, D.C., Sottile, J., and McKeown-Longo, P.J. Activation of distinct alpha5beta1-mediated signaling pathways by fibronectin's cell adhesion and matrix assembly domains. J Cell Biol **141,** 241, 1998.
41. McClay, D., and Hertzler, P.L. Quantitative measurement of cell adhesion using centrifugal force. Current Protocols in Cell Biol **9**, 9.2.1, 1998.
42. Sambrook, J., Fritsch, E.F., and Maniatis, T. Molecular Cloning: A Laboratory Manual. Cold Spring Harbor: Cold Spring Harbor Laboratory Press, 1989.
43. Bae, E., Sakai, T., and Mosher, D.F. Assembly of exogenous fibronectin by fibronectin-null cells is dependent on the adhesive substrate. J Biol Chem **279,** 35749, 2004.
44. Xu, J., Bae, E., Zhang, Q., Annis, D.S., Erickson, H.P., and Mosher, D.F. Display of cell surface sites for fibronectin assembly is modulated by cell adherence to (1)F3 and C-terminal modules of fibronectin. PloS one **4,** e4113, 2009.
45. Hocking, D.C., Sottile, J., Reho, T., Fassler, R., and McKeown-Longo, P.J. Inhibition of fibronectin matrix assembly by the heparin-binding domain of vitronectin. J Biol Chem **274,** 27257, 1999.
46. Sottile, J., Shi, F., Rublyevska, I., Chiang, H.Y., Lust, J., and Chandler, J. Fibronectin-dependent collagen I deposition

modulates the cell response to fibronectin. Am J Physiol Cell Physiol **293,** C1934, 2007.
47. Tuan, R.S., Boland, G., and Tuli, R. Adult mesenchymal stem cells and cell-based tissue engineering. Arthritis Res Ther **5,** 32, 2003.
48. Petrie, T.A., Raynor, J.E., Reyes, C.D., Burns, K.L., Collard, D.M., and Garcia, A.J. The effect of integrin-specific bioactive coatings on tissue healing and implant osseointegration. Biomaterials **29,** 2849, 2008.
49. Garcia, A.J., Huber, F., and Boettiger, D. Force required to break alpha5beta1 integrin-fibronectin bonds in intact adherent cells is sensitive to integrin activation state. J Biol Chem **273,** 10988, 1998.
50. Garcia, A.J., Vega, M.D., and Boettiger, D. Modulation of cell proliferation and differentiation through substrate-dependent changes in fibronectin conformation. Mol Biol Cell **10,** 785, 1999.
51. Zajaczkowski, M.B., Cukierman, E., Galbraith, C.G., and Yamada, K.M. Cell-matrix adhesions on poly(vinyl alcohol) hydrogels. Tissue Eng **9,** 525, 2003.
52. Altroff, H., van der Walle, C.F., Asselin, J., Fairless, R., Campbell, I.D., and Mardon, H.J. The eighth FIII domain of human fibronectin promotes integrin alpha5beta1 binding via stabilization of the ninth FIII domain. J Biol Chem **276,** 38885, 2001.
53. Huveneers, S., and Danen, E.H. Adhesion signaling - crosstalk between integrins, Src and Rho. J Cell Sci **122,** 1059, 2009.
54. Petrie, T.A., Capadona, J.R., Reyes, C.D., and Garcia, A.J. Integrin specificity and enhanced cellular activities associated with surfaces presenting a recombinant fibronectin fragment compared to RGD supports. Biomaterials **27,** 5459, 2006.
55. Barker, T.H. The role of ECM proteins and protein fragments in guiding cell behavior in regenerative medicine. Biomaterials **32,** 4211, 2011.
56. Martino, M.M., Mochizuki, M., Rothenfluh, D.A., Rempel, S.A., Hubbell, J.A., and Barker, T.H. Controlling integrin specificity and stem cell differentiation in 2D and 3D environments through regulation of fibronectin domain stability. Biomaterials **30,** 1089, 2009.
57. Lan, M.A., Gersbach, C.A., Michael, K.E., Keselowsky, B.G., and Garcia, A.J. Myoblast proliferation and differentiation on fibronectin-coated self assembled monolayers presenting different surface chemistries. Biomaterials **26,** 4523, 2005.
58. Salmeron-Sanchez, M., Rico, P., Moratal, D., Lee, T.T., Schwarzbauer, J.E., and Garcia, A.J. Role of material-driven fibronectin fibrillogenesis in cell differentiation. Biomaterials **32,** 2099, 2011.

Address correspondence to:
Denise C. Hocking, PhD
Department of Pharmacology and Physiology
University of Rochester
Box 711
Rochester, NY 14642

E-mail: denise_hocking@urmc.rochester.edu

Received: April 23, 2012
Accepted: September 21, 2012
Online Publication Date: October 30, 2012